Electrochimica Acta 55 (2010) 3471–3476

Contents lists available at ScienceDirect

Electrochimica Acta

journal homepage: www.elsevier.com/locate/electacta

Electrodeposited MnO_2/Au composite film with improved electrocatalytic activity for oxidation of glucose and hydrogen peroxide

Yu Jun Yang [a,b,c], Shengshui Hu [a,b,*]

[a] School of Chemistry and Molecular Sciences, Wuhan University, Wuhan 430072, China
[b] School of Chemistry and Chemical Engineering, Xuchang University, Xuchang 461000, China
[c] State Key Laboratory of Transducer Technology, Chinese Academy of Sciences, China

ARTICLE INFO

Article history:
Received 7 December 2009
Received in revised form 26 January 2010
Accepted 27 January 2010
Available online 2 February 2010

Keywords:
Electrocatalysis
Composite
Enzyme-free sensor
Electrodeposition
Glucose

ABSTRACT

The major drawback of currently used MnO_2 film sensor is the loss of electrical conductivity due to the formation of a poorly conductive MnO_2 layer. To overcome this problem, a coating in which the Au is alloyed with MnO_2 has been developed. The fabrication of the codeposited film electrode of Au and MnO_2 by using a cyclic voltammetric (CV) method was described, and systematic physical and electrochemical characterization was performed. This MnO_2/Au film electrode enhanced MnO_2 electrocatalytic activity. The oxidation process of glucose at the codeposited MnO_2/Au shows a well-defined peak at 0.27 V in alkaline aqueous solution. In contrast, the glucose oxidation at Au modified glassy carbon electrode (GCE) just shows a shoulder wave at 0.42 V. The experimental results indicate that the modification of MnO_2 on the surface of GCE significantly improved the electrocatalytic activity towards the oxidation of glucose. Further study shows that the MnO_2/Au could also effectively catalyze the oxidation of hydrogen peroxide in pH 7.0 phosphate buffer solution (PBS).

1. Introduction

The electrocatalytic oxidation of glucose has been a focal subject of many investigations, because of the great importance of glucose sensing in human blood and their potential use for fuel cell applications [1–5]. Glucose oxidase as enzymatic catalyst has been widely used for glucose biosensor fabrication [6–11]. Good selectivity and high sensitivity have been achieved for glucose detection by enzymatic glucose sensors. However, owing to the nature of enzymes, the most common and serious problem with enzymatic glucose sensors lies in their lack of long-term stability. For instance, the activity of GODx can be easily affected by temperature, pH value, humidity, and toxic chemicals [12–14]. Direct electrocatalytic oxidation of glucose at an enzyme-free electrode would exhibit conveniences and advantages to avoid the drawbacks of the enzyme electrode. Early researches have focused on the use of noble metal-based (containing Pt [15–17] and Au [18]), and alloys-based (containing Pt, Ru, Pb, Au, and Cu [19–25]) electrodes for developing enzyme-free sensors. Various attempts have been made during recent years and modified electrodes made from carbon nanotubes [26], CuO nanowire [27], CuO nanospheres [28] and metallophthalocyanines [29–32] were widely used. It was also reported that MnO_2 with various crystalline structures are promising electrode materials for electrocatalytical oxidation of glucose [33,34].

Hydrogen peroxide is an intermediate or a product in biochemical reactions catalyzed by oxidase. Thus, the monitoring of H_2O_2 with a reliable, rapid and economic method is of great significance [35]. The catalytic effect of MnO_2 towards the oxidation of H_2O_2 was also reported [36–38].

In this article, a new type of catalyst, MnO_2/Au, with enhanced sensing properties of glucose and hydrogen peroxide by taking advantages of MnO_2 [33,34] and Au [18], was prepared by a CV deposition process. This MnO_2/Au film exhibited excellent electrocatalytic activity. It is highly tolerant to chloride ions and generates more stable, reproducible and larger current responses compared with other enzyme-free electrodes. Additionally, electro-oxidation of glucose on such MnO_2/Au surfaces took place at remarkably more negative potentials and, thus, interference could be effectively avoided by detecting glucose at a low potential.

2. Experimental

All chemical reagents used in this experiment were of analytical grade. All solutions were prepared with doubly distilled water. Thin film of MnO_2/Au film was codeposited on GCE by cycling in 2 mM $HAuCl_4$, 10 mM $KMnO_4$ and 0.04 M H_2SO_4 aqueous solution from

* Corresponding author at: College of Chemistry & Molecular Sciences, Wuhan University, Wuhan 430072, China.
E-mail addresses: sshu@whu.edu.cn, cghu@whu.edu.cn, yangyujun418@gmail.com (S. Hu).

0013-4686/$ – see front matter © 2010 Elsevier Ltd. All rights reserved.
doi:10.1016/j.electacta.2010.01.095

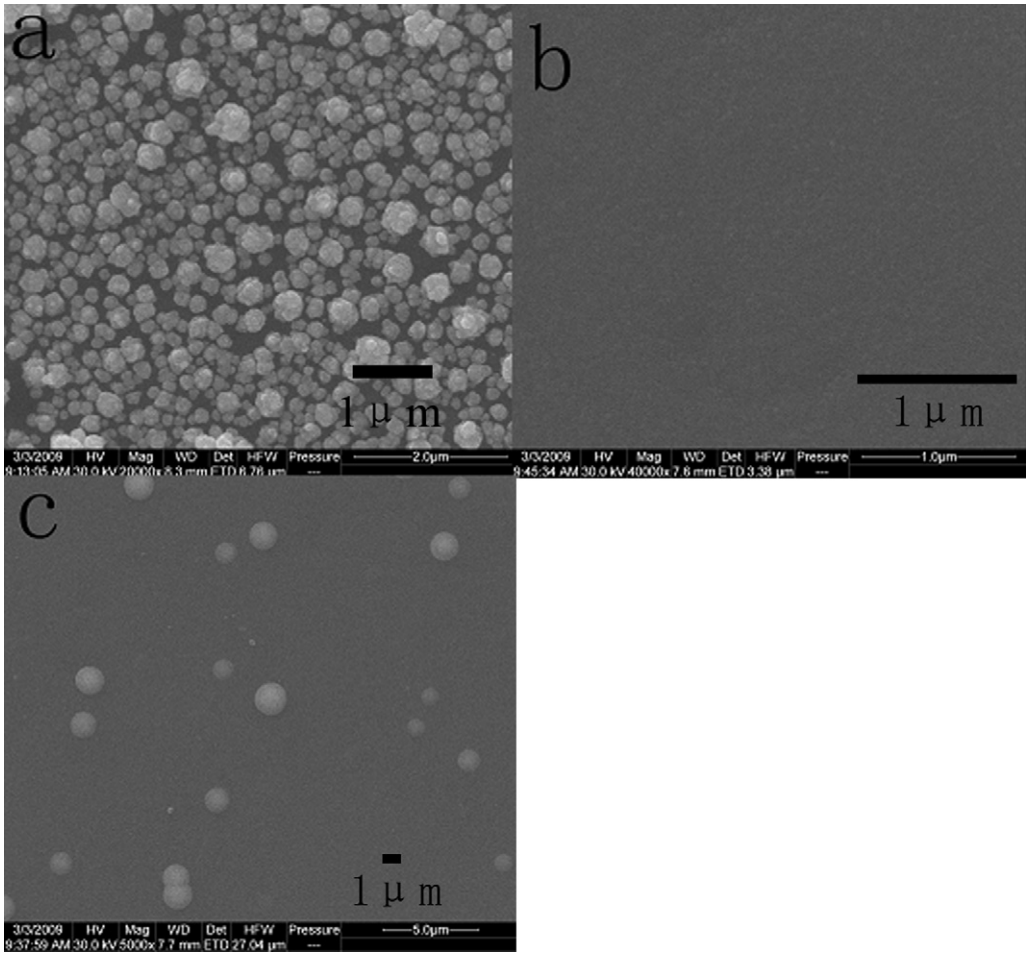

Fig. 1. Scanning electron micrographs of gold (a), MnO_2 (b) and MnO_2/Au (c) electrodeposited on GCE.

0.3 V to −0.5 V at the scan rate of 2 mV s^{-1} for 2 cycles. Au modified GCE (Au/GCE) was prepared by CV in 2 mM $HAuCl_4$, 0.04 M H_2SO_4 solution (from 0.3 V to −0.5 V at the scan rate of 2 mV s^{-1}) for 2 cycles. MnO_2 modified GCE (MnO_2/GCE) was prepared by CV in 6 mM $KMnO_4$, 0.04 M H_2SO_4 solution (from 0.3 V to −0.5 V at the scan rate of 2 mV s^{-1}) for 2 cycles.

A three-electrode electrolytic cell was employed for electrodeposition and electrochemical tests. A GCE (5 mm diameter) was used as the cathode. A platinum wire was used as an anode. The saturated calomel electrode (SCE) was used as a reference electrode. Morphology study of the films on the GCE surface was carried out with a Quanta 200 scanning electron microscope (SEM; FEI Company, Holland). The electrochemical tests were carried out with a CHI 830 potentiostat (Chen Hua Company, China).

3. Results and discussion

Fig. 1 shows the SEM micrographs of the Au, MnO_2 and MnO_2/Au thin films electrodeposited on GCE. The pure Au sample (Fig. 1a) consists of nanoparticles with the average diameter of about 200 nm. The pure MnO_2 sample (Fig. 1b) shows a surface morphology resembling that of the GC substrate, indicating the presence of a continuous MnO_2 film on top of the substrate rather than isolated particles. Fig. 1c corresponding to the codeposited MnO_2/Au catalyst indicates the presence of MnO_2/Au microspheres with the diameter ranging between 200 nm and 1.2 μm.

The deposition mechanism can be attributed to the diffusion and cathodic reduction of anionic MnO_4^- species. The reduction of MnO_4^- species and precipitation of manganese dioxide are in agreement with the Pourbaix diagram for Mn [39]. However, only limited information is available in literature related to the complex chemistry of the reduction of MnO_4^-. The kinetic pathway of reducing Mn^{7+} to Mn^{4+} depends on electrode potential, pH, concentration of MnO_4^- and other species in the solutions [40]. In acidic aqueous solutions the following reaction can result in the reduction

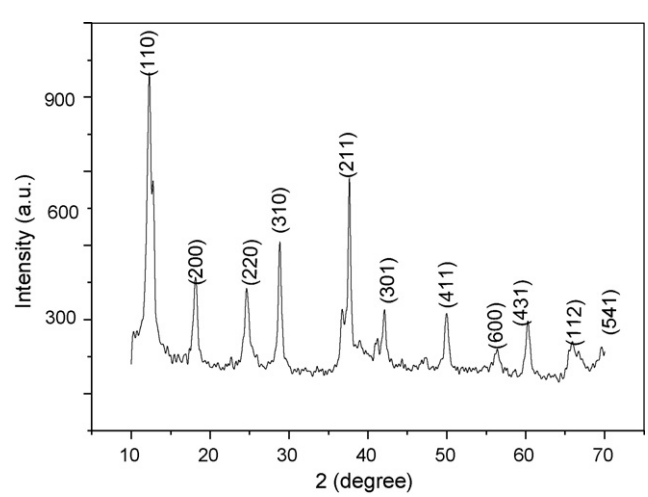

Fig. 2. XRD pattern of the MnO_2 film electrodeposited on GCE.

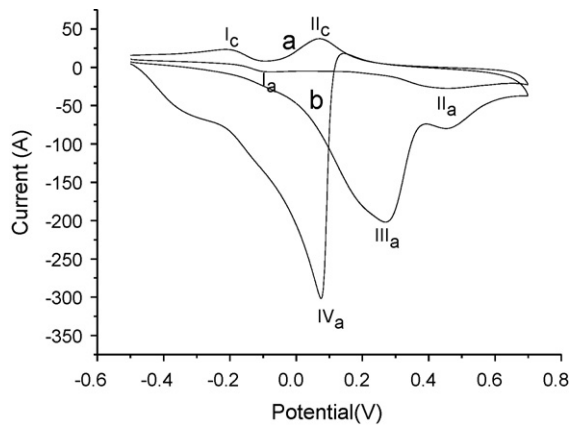

Fig. 3. The CV behaviors of the MnO_2/Au modified GCE in the absence (a) and presence (b) of 10 mM glucose in 0.10 M NaOH solution at 100 mV s^{-1}, scan range: −0.5 V to 0.7 V, initial potential: −0.5 V.

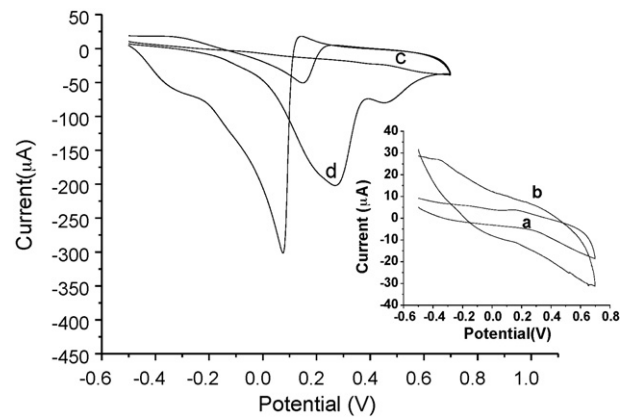

Fig. 4. The CV behaviors of the bare GCE (curve a), MnO_2 modified GCE (curve b), gold modified GCE (curve c) and MnO_2/Au modified GCE (curve d) in 10 mM glucose, 0.1 M NaOH solution at 100 mV s^{-1}, scan range: −0.5 V to 0.7 V, initial potential: −0.5 V.

of MnO_4^- species:

$$MnO_4^- + 4H^+ + 3e^- \rightarrow MnO_2 + 2H_2O \quad (1)$$

Fig. 2 shows a typical XRD pattern of the as-synthesized pure MnO_2 sample. All the reflection peaks can be readily indexed to pure body-centered tetragonal α-MnO_2 phase, with lattice constants of a = 9.816 Å, c = 2.857 Å; which are in agreement with the standard values (JCPDS 44-0141, a = 9.784 Å, c = 2.863 Å). No other phase was detected in the final products.

The electrocatalytic performance of the MnO_2/Au towards the oxidation of glucose was investigated by CV. Fig. 3 shows the CV behaviors of the MnO_2/Au in the absence (a) and presence (b) of 10 mM glucose in 0.10 M NaOH solution. CV of the MnO_2/Au modified GCE in 0.1 M NaOH aqueous solution showed two pairs of redox peaks (curve a). The thin MnO_2 electrodeposited on gold has been studied [41,42] using X-ray photoelectron spectroscopy (XPS), Raman spectroscopy (RS) and electrochemically modulated infrared spectroscopy (EMIRS). Their experimental results indicate that, in borate solutions at pH 9.2, during the MnO_2 reduction, MnO_2 is reduced to Mn(III)OOH while in the reversal positive scan, Mn(III)OOH was oxidized to MnO_2:

$$MnO_2 + H_2O + e = MnOOH + OH^- \quad (2)$$

$$MnOOH + OH^- - e = MnO_2 + H_2O \quad (3)$$

Without the addition of glucose, there is a pair of redox peaks for the MnO_2/Au modified electrode in alkaline solution (Fig. 3a). In the negative scan, MnO_2 was reduced to MnOOH, which was subsequently oxidized to MnO_2 in reversal scan. Two anodic peaks (peak I_a and II_a) can be assigned to the oxidation of MnOOH to Mn(IV), and gold to gold oxide, respectively. Two cathodic peaks (peaks I_c and II_c) can be taken to represent the generation of MnOOH from Mn(IV)

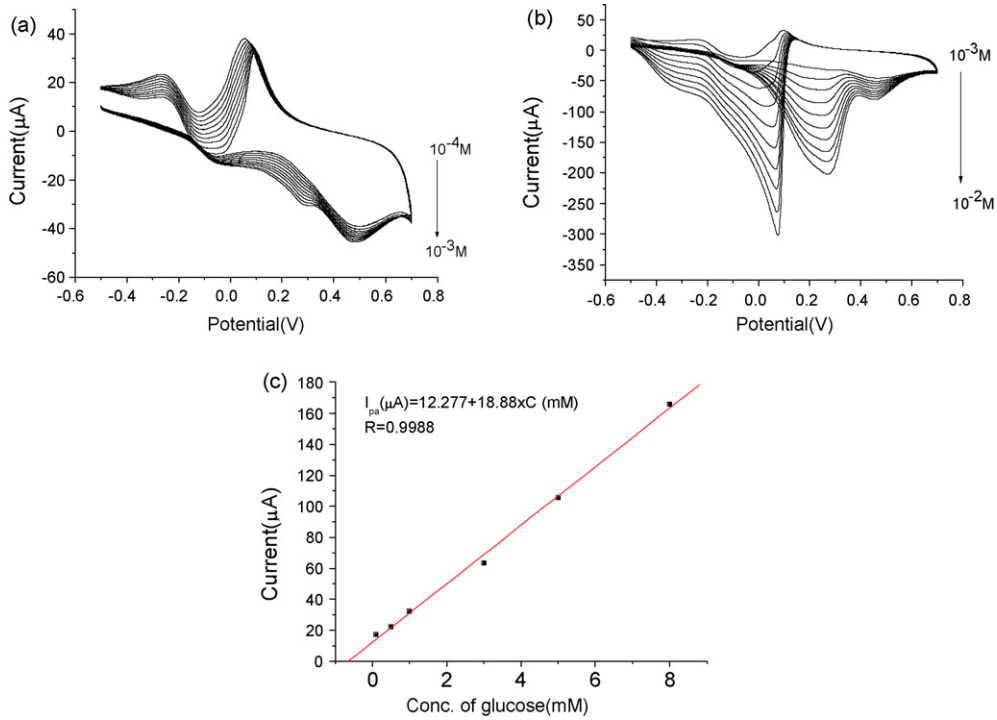

Fig. 5. (a) CVs of MnO_2/Au modified GCE in 0.10 M NaOH solution containing 0.1, 0.2, 0.3, 0.4, 0.5, 0.6, 0.7, 0.8, 0.9 and 1.0 mM glucose at 100 mV s^{-1}; (b) CVs of MnO_2/Au modified GCE in 0.10 M NaOH solution containing 1.0, 2.0, 3.0, 4.0, 5.0, 6.0, 7.0, 8.0, 9.0 and 10.0 mM glucose at 100 mV s^{-1}; (c) the plot of the oxidation peak current with the concentration of glucose.

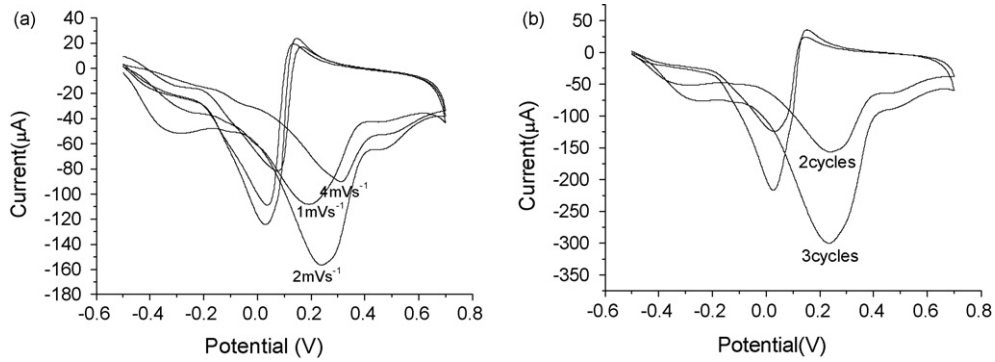

Fig. 6. CVs of MnO_2/Au modified GCEs in 0.10 M NaOH, 0.10 M KCl solution containing 6.0 mM glucose at 100 mV s^{-1}. The MnO_2/Au modified GCEs were prepared in 5 mL deposition bath containing 2 mM $HAuCl_4$, 10 mM $KMnO_4$ and 0.04 M H_2SO_4, scan range: 0.3 V to −0.5 V, initial potential: 0.3 V, (a) at scan rate of 1, 2, and 4 mV s^{-1} for 1, 2, and 4 cycles, respectively and (b) at 2 mV s^{-1} for 1, 2, and 3 cycles.

[43], and gold oxide to gold, respectively [18]. In the presence of glucose, two strong anodic peaks (peak III_a and IV_a) were observed at 0.271 V and 0.076 V (curve b) during the anodic scan and the reverse cathodic scan, respectively while the peak current of peak II_a increased significantly with the addition of glucose. The peak III_a at 0.271 V presents the oxidation process of glucose. Above a potential of +0.3 V, the decrease of current occurs due to the formation of gold oxide, which competes for surface adsorption sites with glucose, also inhibiting the direct electro-oxidation of glucose. In the reverse cathodic scan, with the reduction of the surface gold oxide, enough surface active sites are available for the direct oxidation of glucose, resulting in large peak at around 0.076 V.

The electrocatalytic performance of the bare GCE, Au/GCE, MnO_2/GCE and MnO_2/Au modified GCE (MnO_2/Au/GCE) towards the oxidation of glucose was investigated by CV. Fig. 4 illustrates the CV behaviors of the bare GCE, MnO_2/GCE, Au/GCE, and MnO_2/Au/GCE in 0.10 M NaOH solution containing 10 mM glucose. No current response is observed at the bare GCE (cure a). Because of the loss of electrical conductivity due to the formation of a poorly conductive MnO_2 layer, it is not a surprise to find out that no peak occurs on MnO_2/GCE (curve b). A barely observable anodic peak is obtained at 0.42 V during the anodic scan at the Au/GCE (curve c). In the case of the MnO_2/Au/GCE, three strong anodic peaks are observed at 0.271 V, 0.076 V and 0.45 V (curve d). Like MnO_2/Au/GCE electrode, there is an anodic peak at ~0.2 V during the cathodic scan for Au/GCE electrode too (curve c). The anodic peak at 0.16 V for Au/GCE electrode is also due to the oxidation of glucose [44].

The CVs of the MnO_2/Au electrode in different concentrations of glucose were also measured. Fig. 5a and b shows the standard additions of 100 μM and 1 mM of glucose, respectively, and after each addition the voltammetric response was recorded. These results clearly indicate that, as the concentration of glucose increased, the peak currents of three anodic peaks at 0.271 V, 0.076 V and 0.45 V also increased. The variation of the peak current at 0.271 V *vs.* glucose concentration is linear in the glucose concentration range of 100 μM to 20 mM with a sensitivity and correlation coefficient of 18.9 μA mM^{-1} and 0.9988, respectively. This linear concentration range of 0.1–20 mM is of advantage as the likely glucose level in normal and diabetic person usually varies from 0.2 to 20 mM [45]. The anodic peak at 0.076 V is assigned to the oxidation of glucose. Thus, it is not surprising to find out that the peak current at 0.076 V is also linear with the glucose concentration. The fabrication reproducibility of six biosensors, prepared under the same conditions, showed an acceptable reproducibility with a R.S.D. of 3.2% for the peak current obtained in the glucose concentration of 1.0 mM. The results indicate that the MnO_2/Au electrode has a good operational stability. The activity of the electrode retained almost its initial current response after it was stored at room temperature for 30 days, indicating the excellent stability of the sensor. These results demonstrate that the MnO_2/Au electrode is very efficient for the determination of glucose.

As shown in Fig. 4, MnO_2 in the MnO_2/Au plays a crucial role for the oxidation of glucose. The catalytic effect of MnO_2 towards the oxidation of glucose is probably due to a parallel catalytic reaction. As soon as MnO_2 is reduced to lower valence states by glucose, it is electro-oxidized back to MnO_2 at the electrode surface. The catalytic mechanism of gold towards the oxidation of glucose in alkaline solution may be described as following [18]:

$$Au + OH^- = AuOH + e \quad (4)$$

$$AuOH + CHO(CHOH)_4CH_2OH \xrightarrow{OH^-} COOH(CHOH)_4CH_2OH + Au + H_2O + e \quad (5)$$

Therefore, MnO_2 and gold act not only as the electron mediate but as catalyst as well [33]. Studies on the SEM of MnO_2/Au/GCE (Fig. 1c) and Au (Fig. 1b) further confirm our assumption that the improvement in catalytic activity is attributed to catalytic effects of MnO_2 and gold rather than any physical effects (such as increase in surface area).

The effects of scan rate and number of scan cycles during the CV deposition process on the catalytic oxidation of glucose were also investigated. As shown in Fig. 6a, the oxidation peak shifted positively as the scan rate is increased from 1 to 2 and 4 mV s^{-1}

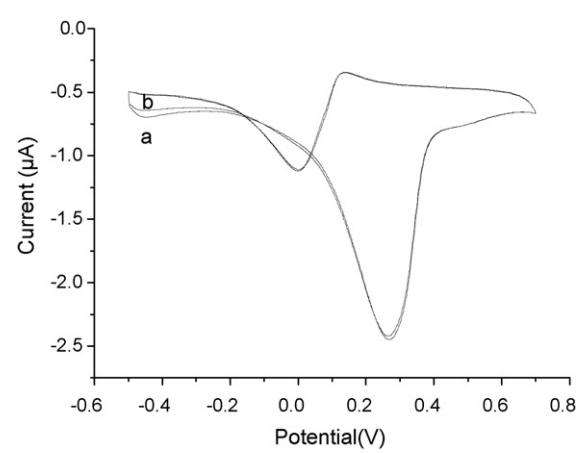

Fig. 7. (a) CVs of MnO_2/Au modified GCE in 0.10 M NaOH, 0.10 M KCl solution containing 6.0 mM glucose at 100 mV s^{-1} and (b) CVs of MnO_2/Au modified GCE in 0.10 M NaOH solution containing 6.0 mM glucose at 100 mV s^{-1}.

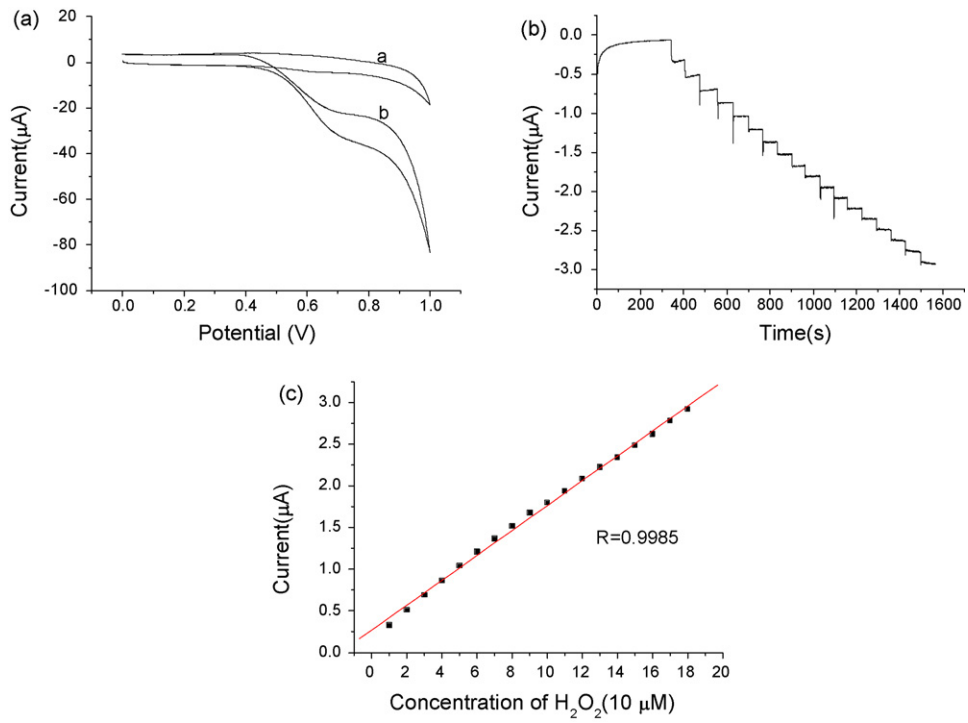

Fig. 8. (a) CVs of H_2O_2 on MnO_2/Au/GCE in PBS (pH 7.0) in the absence (curve a) and presence of 10 mM H_2O_2 (curve b). Scan rate: 100 mV s^{-1}; (b) dynamic current responses of MnO_2/Au/GCE to successive addition of H_2O_2 at pH 7.0. Inject 20 μL 5×10^{-2} M H_2O_2 solution into 10 mL PBS (pH 7.0) with a microsyringe. The concentration change of H_2O_2 is 10 μM per addition. Applied potential: 0.70 V; (c) calibration curve of H_2O_2 amperometric biosensor based on MnO_2/Au/GCE in PBS buffer (pH 7.0). Applied potential 0.70 V.

while the highest peak current is obtained at 2 mV s^{-1}. At 2 mV s^{-1}, the oxidation current is increased significantly with increasing the number of scan cycles from 2 to 3 cycles (Fig. 6b). However the obtained film will be too thick and easy to crack when the GCE was scanned for 3 cycles in the plating bath. Thus, the number of scan adopted in this experiment is 2 cycles.

To evaluate the selectivity of the proposed biosensor, three possible interfering biomolecules, ascorbic acid (AA), dopamine (DA), and uric acid (UA), which normally coexist with glucose in real samples (human blood) were examined [46]. Considering that the concentration of glucose in the human blood is about 30 times of AA, DA or UA, the voltammetric response of the MnO_2/Au towards the addition of 1 mM glucose and 0.1 mM AA, DA, and UA was examined in 0.10 M NaOH solution and the $i_{glucose+interferent}/i_{glucose}$ is 103%, 99% and 98%, respectively. To sum up, the selectivity was improved so much on this enzyme-free biosensor that the three common interfering biomolecules, AA, DA, and UA caused negligible interference to the response of glucose at the MnO_2/Au electrode.

Electrodes based on metals [15,17] or alloys [18,24] towards the oxidation of glucose usually lose their activity due to the poisoning of chloride ions [19]. In order to understand whether chloride ions will poison the MnO_2/Au electrode, the CV was measured in the solution with high concentration of chloride ions (i.e., replacing 0.10 M NaOH with 0.10 M KCl + 0.10 M NaOH as the electrolyte). The current response of MnO_2/Au/GCE towards glucose oxidation remains almost unchanged (Fig. 7), implying that the MnO_2/Au/GCE is also highly resistant to poisoning by chloride ions and can be used as a glucose sensor even in the presence of high concentration of chloride ions.

Fig. 8a shows the CVs for hydrogen peroxide with the prepared MnO_2/Au modified GCE. In the absence of hydrogen peroxide, there is a pair of very broad but barely observable waves between 0.2 V and 0.8 V (curve a) in PBS solution. It may be assigned to the reduction of MnO_2 to Mn(II,III) and the reoxidation of Mn(II,III) back to MnO_2 [36]. In the presence of H_2O_2, the CV displays a very significant oxidative current at potentials between 0.5 V and 1.0 V (curve b). The current for the oxidation of Mn(II,III) to MnO_2 significantly increases with increasing H_2O_2 concentration. The characteristic shape of the CV in this potential region indicates that the signal is probably due to a parallel catalytic reaction. As soon as MnO_2 is reduced to lower states by H_2O_2, it is electro-oxidized back to MnO_2 at the electrode surface [36]:

$$MnO_2 + H_2O_2 \rightarrow MnO \quad (\text{or} \quad Mn_2O_3) + O_2 + H_2O \tag{6}$$

$$MnO \quad (\text{or} \quad Mn_2O_3) \rightarrow MnO_2 + 2e \tag{7}$$

Since the above two reactions are fast, the parallel current is much higher than the oxidation current of MnO_2 on the electrode surface without H_2O_2. Effect of applied potential on the amperometric response of 10 μM H_2O_2 in phosphate buffer solution was studied. Although at 0.80 V the signal is highest, we choose 0.70 V as the operating potential because above 0.70 V there is increased noise, which is a disadvantage for measuring low H_2O_2 concentrations. The relationship between the oxidation current and the concentration of H_2O_2 was examined in a PBS solution (pH 7.0). The solution was stirred to ensure uniform distribution of H_2O_2 in the cell. Fig. 8b displays the amperometric response for the H_2O_2. When the same amount of H_2O_2 was injected into the cell, the concentration change of H_2O_2 in the cell is 10 μM per addition and the current was recorded instantly. Calibration curves for H_2O_2 measurement are also presented in Fig. 8c. The current is linear for concentrations of H_2O_2 from 5×10^{-6} to 1×10^{-2} M. The upper limit of linearity range (10^{-2} M) was attained by examining the relationship between the oxidation current and the concentration of H_2O_2 after injecting same amount of H_2O_2 (concentration change: 5×10^{-4} M/addition) into the cell. The sensitivity of the sensor to H_2O_2 was calculated to be 1.49×10^4 μA M^{-1}. The detection limit was estimated to be 1×10^{-6} M (signal/noise = 3).

4. Conclusion

In this work we have been able to synthesize MnO_2/Au on the surface of GCE *via* a simple CV codeposition method. The size and morphology of the sample was investigated through the use of FE-SEM showing the sample to consist of MnO_2/Au nanoclusters. These MnO_2/Au modified GCEs can be used in the catalytic oxidation of glucose and hydrogen peroxide. This novel MnO_2/Au composite film is a potential candidate for application in terms of fuel cells and enzyme-free sensors.

Acknowledgement

The authors acknowledge financial support by the National Nature Science Foundation of China (Nos. 30770549, 20805035 and 90817103).

References

[1] J.L.C. Clark, C. Lyons, A.N.Y. Aead, Science 102 (1962) 29.
[2] G. Reach, G.S. Wilson, Anal. Chem. 64 (1992) 381A.
[3] A.P.F. Turner, B. Chen, A.P. Sergey, Clin. Chem. 45 (1999) 1596.
[4] E. Katz, I. Willner, A.B. Kotlyar, J. Electroanal. Chem. 479 (1999) 64.
[5] N. Mano, F. Mao, A. Heller, J. Am. Chem. Soc. 125 (2003) 6588.
[6] X.H. Kang, Z.B. Mai, X.Y. Zou, P.X. Cai, J.Y. Mo, Anal. Biochem. 369 (2007) 71.
[7] S.G. Wang, Q. Zhang, R.L. Wang, S.F. Yoon, J. Ahn, D.J. Yang, Electrochem. Commun. 5 (2003) 800.
[8] H. Tang, J.H. Chen, S.Z. Yao, L.H. Nie, G.H. Deng, Y.F. Kuang, Anal. Biochem. 331 (2004) 89.
[9] X. Chu, D.X. Duan, G.L. Shen, R.Q. Yu, Talanta 71 (2007) 2040.
[10] Y.J. Zou, C.L. Xiang, L.X. Sun, F. Xu, Biosens. Bioelectron. 23 (2008) 1010.
[11] Y.C. Tsai, S.C. Li, J.M. Chen, Langmuir 21 (2005) 3653.
[12] R. Wilson, A.P.F. Turner, Biosens. Bioelectron. 7 (1992) 165.
[13] F. Shoji, M.S. Freund, J. Am. Chem. Soc. 123 (2001) 3383.
[14] S.J. Park, H.K. Boo, T.D. Chung, Anal. Chim. Acta 556 (2006) 46.
[15] B. Beden, F. Largeaud, K.B. Kokoh, C. Lamy, Electrochim. Acta 41 (1996) 701.
[16] A.N. Gracea, K. Pandian, J. Phys. Chem. Solids 68 (2007) 2278.
[17] X.H. Kang, Z.B. Mai, X.Y. Zou, P.X. Cai, J.Y. Mo, Talanta 74 (2008) 879.
[18] M. Tominaga, T. Shimazoe, M. Nagashima, H. Kusuda, A. Kubo, Y. Kuwahara, I. Taniguchi, J. Electroanal. Chem. 590 (2006) 37.
[19] Y.P. Sun, H. Buck, T.E. Mallouk, Anal. Chem. 73 (2001) 1599.
[20] R. Qiu, X.L. Zhang, R. Qiao, Y. Li, Y.I. Kim, Y.S. Kang, Chem. Mater. 19 (2007) 4174.
[21] S.B. Aoun, Z. Dursun, T. Koga, G.S. Bang, J. Electroanal. Chem. 567 (2004) 175.
[22] H.F. Cui, J.S. Ye, X. Liu, W.D. Zhang, F.S. Sheu, Nanotechnology 17 (2006) 2334.
[23] C.C. Jin, Z.D. Chen, Synth. Met. 157 (2007) 592.
[24] J.P. Wang, D.F. Thomas, A.C. Chen, Anal. Chem. 80 (2008) 997.
[25] Y. Bai, Y.Y. Sun, C.Q. Sun, Biosens. Bioelectron. 24 (2008) 579.
[26] J.S. Ye, Y. Wen, W.D. Zhang, L.M. Gan, G.Q. Xu, F.S. Sheu, Electrochem. Commun. 6 (2004) 66.
[27] Z.J. Zhuang, X.D. Su, H.Y. Yuan, Q. Sun, D. Xiao, M.M.F. Choi, Analyst 33 (2008) 126.
[28] E. Reitz, W.Z. Jia, M. Gentile, Y. Wang, Y. Lei, Electroanalysis 20 (2008) 2482.
[29] C. Barrera, I. Zhukov, E. Villagra, F. Bedioui, M.A. Paez, J. Costamagna, J.H. Zagal, J. Electroanal. Chem. 589 (2006) 212.
[30] K.I. Ozoemena, T. Nyokong, Electrochim. Acta 51 (2006) 5131.
[31] P.N. Mashazi, K.I. Ozoemena, T. Nyokong, Electrochim. Acta 52 (2006) 177.
[32] L. Ozcan, Y. Sahin, H. Turk, Biosens. Bioelectron. 24 (2008) 512.
[33] D. Das, P.K. Sen, K. Das, J. Electroanal. Chem. 611 (2007) 19.
[34] J. Chen, W.D. Zhang, J.S. Ye, Electrochem. Commun. 10 (2008) 1268.
[35] K. Schachl, H. Alemu, K. Kalcher, I. Svancara, K. Vytras, Analyst 122 (1997) 985.
[36] S.J. Yao, S. Yuan, J.H. Xu, Y. Wang, J.L. Luo, S.S. Hu, Appl. Clay Sci. 33 (2006) 35.
[37] X.W. Zheng, Z.H. Guo, Talanta 50 (2000) 1157.
[38] K. Schachl, H. Alemu, K. Kalcher, H. Moderegger, I. Svancara, K. Vytras, Fresenius J. Anal. Chem. 362 (1998) 194.
[39] A. Moussard, J. Brenet, F. Jolas, M. Pourbaix, J. van Muylder, in: M. Pourbaix (Ed.), Atlas of Electrochemical Equilibria in Aqueous Solutions, National Association of Corrosion Engineers, Pergamon Press, Oxford, 1974.
[40] J. Wei, I. Zhitomirsky, Surf. Eng. 24 (2008) 45.
[41] B.A. Lopez de Mishima, T. Ohtsuka, K. Konno, N. Sato, Electrochim. Acta 36 (1991) 1458.
[42] B.A. Lopez de Mishima, T. Ohtsuka, N. Sato, Electrochim. Acta 38 (1993) 341.
[43] C. Batchelor-McAuley, L. Shao, G.G. Wildgoose, M.L.H. Green, R.G. Compton, New J. Chem. 32 (2008) 1195.
[44] M.P. Bui, S. Lee, K.N. Han, X.H. Pham, C.A. Li, J. Choo, G.H. Seong, Chem. Commun. (2009) 5549.
[45] B.R. Eggins, Chemical Sensors and Biosensors, John Wiley & Sons, UK, 2003.
[46] B.H. Liu, R.Q. Hu, J.Q. Deng, Anal. Chem. 69 (1997) 2343.